

# Pan-Arctic land–atmospheric fluxes of methane and carbon dioxide in response to climate change over the 21st century

Xudong Zhu<sup>1</sup>, Qianlai Zhuang<sup>1,2</sup>, Xiang Gao<sup>3</sup>, Andrei Sokolov<sup>3</sup> and C Adam Schlosser<sup>3</sup>

<sup>1</sup> Department of Earth, Atmospheric and Planetary Sciences, Purdue University, West Lafayette, IN 47907, USA

<sup>2</sup> Department of Agronomy, Purdue University, West Lafayette, IN 47907, USA

<sup>3</sup> MIT Joint Program on the Science and Policy of Global Change, Massachusetts Institute of Technology, Cambridge, MA 02139, USA

E-mail: [zhu123@purdue.edu](mailto:zhu123@purdue.edu)

Received 2 April 2013

Accepted for publication 19 September 2013


Published 4 October 2013

Online at [stacks.iop.org/ERL/8/045003](http://stacks.iop.org/ERL/8/045003)

## Abstract

Future changes of pan-Arctic land–atmospheric methane (CH<sub>4</sub>) and carbon dioxide (CO<sub>2</sub>) depend on how terrestrial ecosystems respond to warming climate. Here, we used a coupled hydrology–biogeochemistry model to make our estimates of these carbon exchanges with two contrasting climate change scenarios (no-policy versus policy) over the 21st century, by considering (1) a detailed water table dynamics and (2) a permafrost-thawing effect. Our simulations indicate that, under present climate conditions, pan-Arctic terrestrial ecosystems act as a net greenhouse gas (GHG) sink of  $-0.2 \text{ Pg CO}_2\text{-eq. yr}^{-1}$ , as a result of a CH<sub>4</sub> source ( $53 \text{ Tg CH}_4 \text{ yr}^{-1}$ ) and a CO<sub>2</sub> sink ( $-0.4 \text{ Pg C yr}^{-1}$ ). In response to warming climate, both CH<sub>4</sub> emissions and CO<sub>2</sub> uptakes are projected to increase over the century, but the increasing rates largely depend on the climate change scenario. Under the non-policy scenario, the CH<sub>4</sub> source and CO<sub>2</sub> sink are projected to increase by 60% and 75% by 2100, respectively, while the GHG sink does not show a significant trend. Thawing permafrost has a small effect on GHG sink under the policy scenario; however, under the no-policy scenario, about two thirds of the accumulated GHG sink over the 21st century has been offset by the carbon losses as CH<sub>4</sub> and CO<sub>2</sub> from thawing permafrost. Over the century, nearly all CO<sub>2</sub>-induced GHG sink through photosynthesis has been undone by CH<sub>4</sub>-induced GHG source. This study indicates that increasing active layer depth significantly affects soil carbon decomposition in response to future climate change. The methane emissions considering more detailed water table dynamics continuously play an important role in affecting regional radiative forcing in the pan-Arctic.

**Keywords:** methane, carbon dioxide, greenhouse gases, climate change, Arctic, terrestrial ecosystem model, variable infiltration capacity

 Online supplementary data available from [stacks.iop.org/ERL/8/045003/mmedia](http://stacks.iop.org/ERL/8/045003/mmedia)



Content from this work may be used under the terms of the [Creative Commons Attribution 3.0 licence](http://creativecommons.org/licenses/by/3.0/). Any further distribution of this work must maintain attribution to the author(s) and the title of the work, journal citation and DOI.

## 1. Introduction

Future changes in carbon stocks of pan-Arctic terrestrial ecosystems in response to climate change are mainly determined by the increases in net primary productivity (NPP),

during warmer and longer growing seasons (Euskirchen *et al* 2006), and in heterotrophic respiration ( $R_h$ ), in warmer and deeper soil active layers (Hollesen *et al* 2011). The soil organic carbon (SOC) of terrestrial ecosystems in pan-Arctic permafrost region (~16% of the global soil area) is estimated to be about 50% of the global SOC (Tarnocai *et al* 2009). The disproportionately large SOC has been accumulated historically due to slow decomposition rate with low temperature, but warmer and wetter future climate may accelerate soil biogeochemical cycling, leading to loss of carbon (Webster *et al* 2003, ACIA 2004, Davidson and Janssens 2006). Warming and thawing permafrost results in thicker soil active layers, which could lead to both enhanced decomposition and plant growth (Mack *et al* 2004), and previously frozen soil carbon is being converted and released as  $CH_4$  and  $CO_2$  (Harden *et al* 2012), which, as two major greenhouse gases (GHG), may significantly feedback to climate given the large size of SOC and warming climate in the pan-Arctic (Schuur *et al* 2008).

The uncertainty in boreal carbon budgets and their responses to climate change over the 21st century are among the largest remaining gaps in assessing regional carbon dynamics in pan-Arctic terrestrial ecosystems (e.g., McGuire *et al* 2009, Koven *et al* 2011). To date, the amounts and rates of land-atmospheric  $CH_4$  and  $CO_2$  fluxes are poorly constrained, as is the ratio of  $CH_4$  to  $CO_2$  (e.g., Whiting and Chanton 2001). The ratio, as an index of land-atmospheric GHG carbon exchange (Gorham 1991), is important in terms of carbon-climate feedbacks given higher radiative efficiency of  $CH_4$ . The relative amount of  $CH_4$  and  $CO_2$  released from soil carbon mineralization depends on the amount of available oxygen or dry/wet conditions in the soil (Segers 1998). More future precipitation and thermokarst may result in wetter soil conditions (Walter *et al* 2006), which favor  $CH_4$  production, while water redistribution towards thermokarst depressions may lead to drier soils in adjacent higher areas (Osterkamp *et al* 2009), which favor  $CO_2$  production. Thus, how the quantity and quality (i.e., the ratio of  $CH_4$  to  $CO_2$ ) of regional carbon budgets will change over the 21st century depends on how pan-Arctic terrestrial ecosystems respond to potentially dramatic environmental changes, including rising temperature, change of precipitation regimes, and resultant changes in soil thermal and hydrological conditions (Romanovsky *et al* 2007, Schulze *et al* 2001, Zhuang *et al* 2006, Solomon *et al* 2007).

To evaluate regional carbon budgets of  $CH_4$  and  $CO_2$  and their respective impacts on climate radiative forcing, the net methane exchanges (NME) and net ecosystem exchange (NEE) need to be quantified. To date, most regional carbon dynamics studies focus on either NME (e.g., Walter *et al* 2001, Melton *et al* 2013) or NEE (e.g., Clein *et al* 2002, Carrasco *et al* 2006). Only a few process-based models were developed to simulate both NME and NEE at region scales, but they assumed uniform water table depth (WTD) over large grid cells (e.g.,  $0.5^\circ$ ) without considering the sub-grid spatial heterogeneity of water table dynamics (e.g., Zhuang *et al* 2006), which is important in the quantification of regional carbon budgets (Bohn and Lettenmaier 2010). In

this study, we used a coupled hydrology–biogeochemistry model framework, incorporating sub-grid spatial variation in the WTD, to estimate land–atmospheric NME and NEE over the pan-Arctic during the 21st century. We have three main objectives: (1) to explore how NME and NEE respond to future climate change, (2) to analyze the relative contribution of  $CH_4$  and  $CO_2$  to regional carbon budgets and radiative forcing, (3) to examine the effects of permafrost thawing on projected regional carbon dynamics.

## 2. Methods

### 2.1. Model and data

A macro-scale hydrological model (variable infiltration capacity, VIC Liang *et al* 1994, Cherkauer *et al* 2003) and a biogeochemical model (terrestrial ecosystem model, TEM Raich *et al* 1991, Zhuang *et al* 2004) were coupled (figure 1) to make estimates of land–atmospheric NME and NEE over the pan-Arctic, which is defined as the watersheds of major rivers that drain into the Arctic Ocean (Lammers *et al* 2001). This coupled VIC–TEM model framework was developed and applied to estimate NME (Lu and Zhuang 2012). Here, we extended the model framework to estimate both NME and NEE. The VIC model simulates soil thermal and hydrological dynamics using physically based formulations (Liang *et al* 1994), and has been applied in cold region hydrology (Su *et al* 2005, 2006) by the incorporation of a frozen soil/permafrost algorithm (Cherkauer *et al* 2003). The TEM model explicitly simulates carbon and nitrogen dynamics of vegetation and soils, and has been used to examine terrestrial  $CH_4$  and  $CO_2$  dynamics in high latitudes (Zhuang *et al* 2004, 2006, McGuire *et al* 2010). TEM has its hydrological module (Zhuang *et al* 2002) to simulate water dynamics of terrestrial ecosystems. However, like many existing biogeochemistry models, the hydrological module is formulated as a simple ‘single-bucket’. To improve the estimates of soil moisture profile, a key controlling factor for biogeochemical processes of  $CH_4$  and  $CO_2$ , more sophisticated hydrological models, like VIC, are needed (e.g., Bohn and Lettenmaier 2010, Lu and Zhuang 2012). In TEM, the NME is calculated as the difference between  $CH_4$  production (methanogenesis) and  $CH_4$  oxidation (methanotrophy). The NEE is calculated as the difference between  $CO_2$  uptakes, through plant photosynthesis, and  $CO_2$  emissions, from  $R_h$  and accompanied releases of  $CO_2$  associated with methanogenesis and methanotrophy (Conrad *et al* 1989, Tang *et al* 2010). The size of SOC pool in TEM is determined by the balance between litter production (proportional to vegetation carbon pool) and  $R_h$ . To consider the effect of thawing permafrost on carbon dynamics, a permafrost-switch was set in this study to control the newly available SOC due to permafrost thawing. When the permafrost-switch was on, the newly available SOC was simply added into SOC pool of the TEM once in a year (at the end of each year). When the switch was off, this effect was deactivated. The magnitude of newly available SOC was calculated based on the annual change of simulated active layer depth (ALD) weighted by spatially

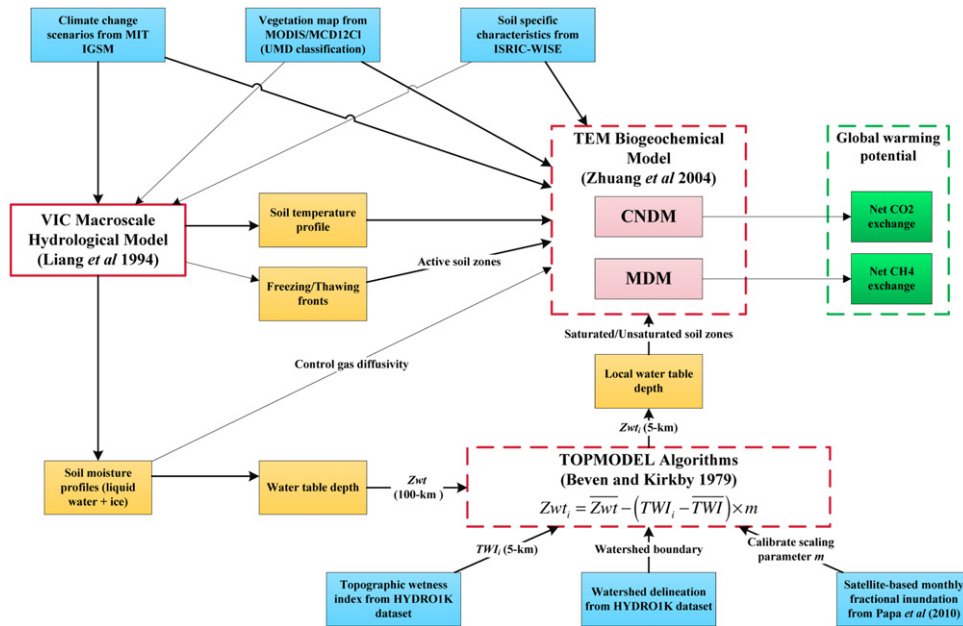


**Figure 1.** Conceptual framework of coupled models to estimate net fluxes of methane and carbon dioxide. Shown are external spatial inputs (blue) for driving or calibrating models, internal information exchange (yellow) between models, and final model outputs (green). Arrows indicate the direction of information exchange among all components. See text and supplementary materials for details (available at [stacks.iop.org/ERL/8/045003/mmedia](http://stacks.iop.org/ERL/8/045003/mmedia)).

explicit SOC profiles derived from Harden *et al* (2012) (see the supplementary materials for details, available at [stacks.iop.org/ERL/8/045003/mmedia](http://stacks.iop.org/ERL/8/045003/mmedia)).

This study used two contrast climate change scenarios simulated by the MIT’s integrated global systems model (IGSM) (Reilly *et al* 1999, Prinn *et al* 1999, Webster *et al* 2003, Sokolov *et al* 2009) with a median transient climate response (Webster *et al* 2012): a no-policy scenario (a reference case assuming no explicit climate policy) and a policy scenario (a stabilization case assuming a specified climate policy). The projected atmospheric CO<sub>2</sub> mole fraction (parts per million, ppm) in 2100 is about 900 ppm and 480 ppm for no-policy and policy scenarios, respectively. Air temperature over the region is projected to increase by 8 °C and 2 °C, and annual precipitation is projected to increase by 200 mm and 70 mm, respectively. Further details on climate change scenarios and all other spatially explicit inputs (figure 1) for the VIC–TEM model framework are provided in the supplementary materials.

## 2.2. Simulation protocol

In the VIC–TEM model framework, the VIC model was first run to solve soil moisture and energy balance and provide soil freeze/thaw fronts, soil temperature, ice and moisture profiles. All these VIC outputs were fed directly into TEM model except soil moisture profile, which was used to estimate WTD using the soil moisture deficit method (Bohn *et al* 2007) and then fed into the TEM model after redistributing WTD based on a TOPMODEL parameterization scheme (see the supplementary materials). To examine how NME and NEE respond to future climate change, we conducted two model

simulations over the 21st century using future atmospheric CO<sub>2</sub> concentrations and climate forcing from each of the two climate change scenarios: no-policy and policy scenarios. The permafrost-thawing effect was considered in the simulations by turning on the permafrost-switch. The spatio-temporal dynamics of NME and NEE over the pan-Arctic and their relative impacts on climate system were analyzed based on these two model simulations: no-policy and policy simulation. The warming/cooling impacts of NME and NEE on climate system were compared using the global warming potentials (GWP) (denoted as CO<sub>2</sub>-eq.), assuming one gram of CH<sub>4</sub> is equivalent to 25 g of CO<sub>2</sub> over a 100-year time horizon (Solomon *et al* 2007). In addition, in order to separate the effects of permafrost thawing from others, we conducted another two model simulations using the same two scenarios but with the permafrost-switch turned off. We calculated the effect of permafrost thawing as the difference between the two sets of simulations with and without considering the permafrost-thawing effect.

## 3. Results and discussion

### 3.1. Spatial patterns of CH<sub>4</sub> and CO<sub>2</sub> fluxes

Both NME and NEE estimates showed substantial spatial variations over the region, with consistent spatial patterns between no-policy (figures 2(a)–(d)) and policy (figures S1(a)–(d), available at [stacks.iop.org/ERL/8/045003/mmedia](http://stacks.iop.org/ERL/8/045003/mmedia)) simulations. As indicated by the mean annual estimates of the 2000s and 2090s, the spatial patterns of both NME and NEE seemed not to change over time for each simulation. The highest positive NME, or CH<sub>4</sub> source, occurred in the



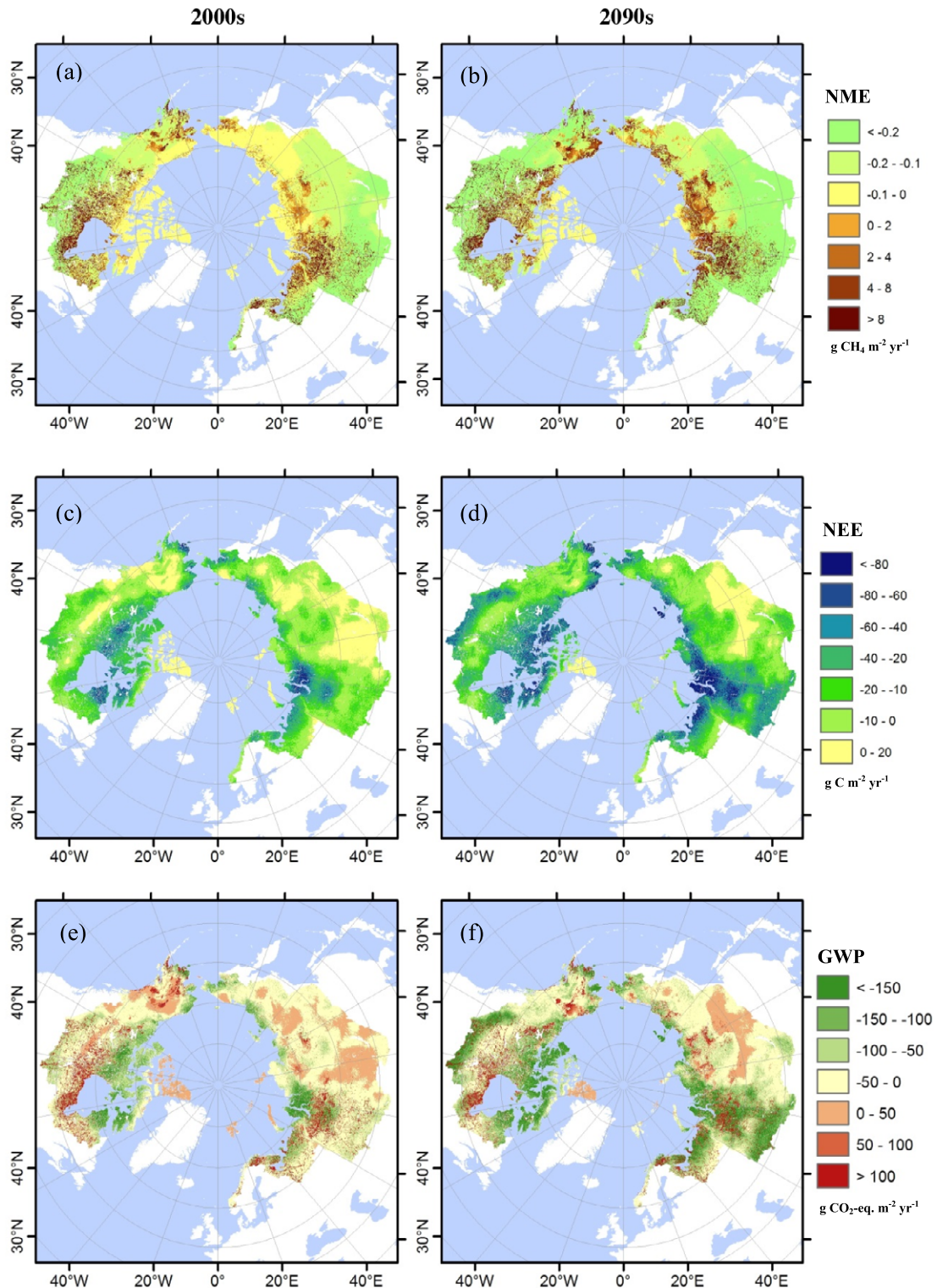


**Figure 2.** Mean annual net methane exchange (NME) (top row), net ecosystem exchange (NEE) (middle row), and net global warming potential (GWP) (bottom row) over the pan-Arctic during the 2000s (left column) and the 2090s (right column), under the no-policy scenario.

West Siberian Lowlands and the Hudson Bay Lowlands, with CH<sub>4</sub> sources up to 8 g CH<sub>4</sub> m<sup>-2</sup> yr<sup>-1</sup> during the 2000s. The negative NME, or CH<sub>4</sub> sink, existed over the southern parts of the study region, with CH<sub>4</sub> sinks up to -0.2 g CH<sub>4</sub> m<sup>-2</sup> yr<sup>-1</sup> during the 2000s.

The magnitude and spatial variations of NME were generally consistent with previous regional CH<sub>4</sub> studies focusing on northern high latitudes (e.g., Zhuang *et al* 2004, Petrescu *et al* 2010, Zhu *et al* 2011). In terms of the similarity in spatial patterns, the CH<sub>4</sub> sinks seemed to

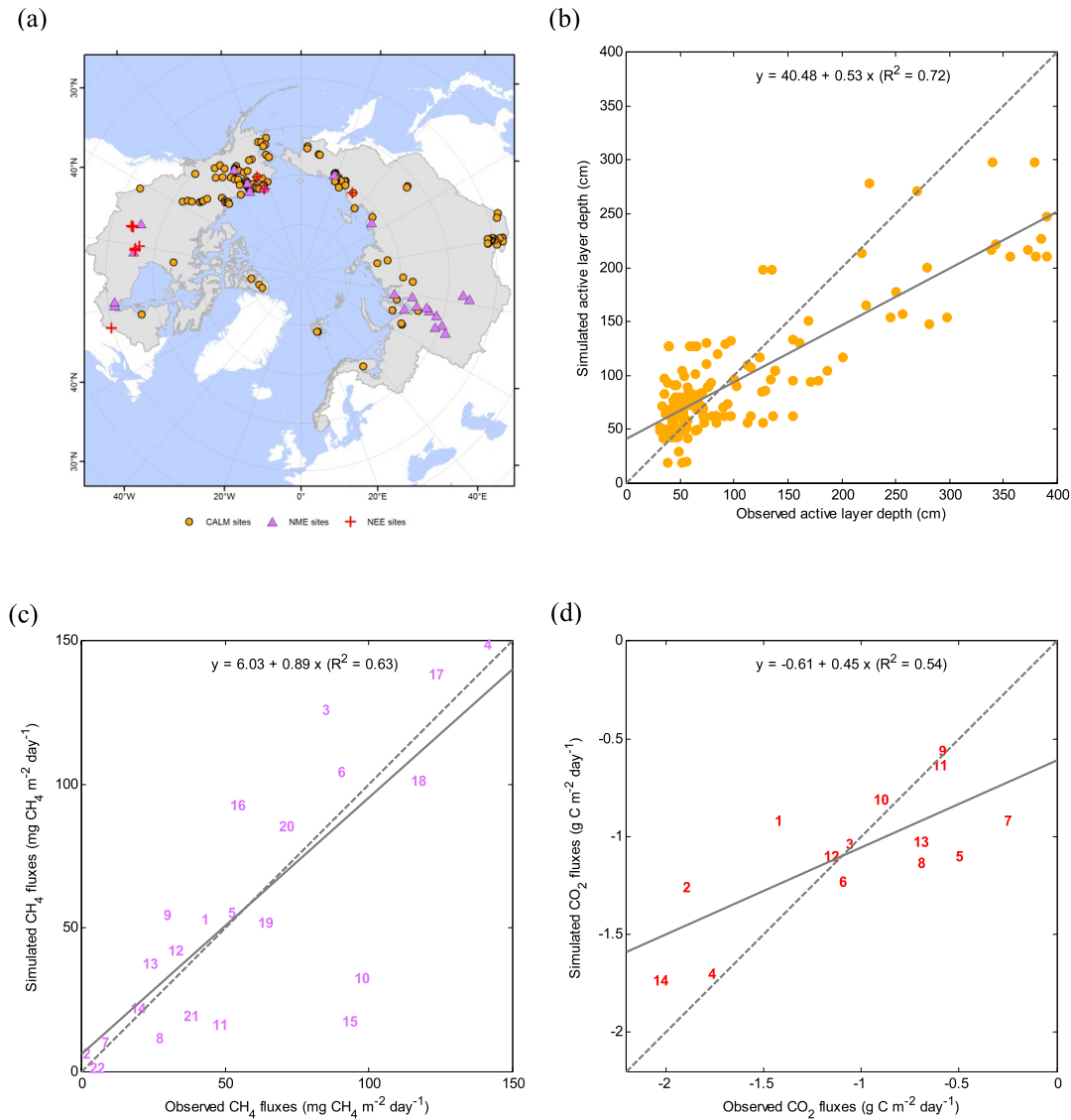


**Figure 3.** Comparison of the observed and simulated active layer depths (b), CH<sub>4</sub> fluxes (c), and CO<sub>2</sub> fluxes (d) at field sites over the pan-Arctic (a). The observed active layer depths are multi-year mean values of annual end-of-season thaw depth from 155 circumpolar active layer monitoring (CALM) sites (Brown *et al* 2000). The observed net fluxes of CH<sub>4</sub> and CO<sub>2</sub> are mean daily fluxes during the growing season (May–Sep.), and the information of 22 CH<sub>4</sub> flux sites and 14 CO<sub>2</sub> flux sites can be found in tables S1 and S2 (available at [stacks.iop.org/ERL/8/045003/mmedia](http://stacks.iop.org/ERL/8/045003/mmedia)), respectively. Solid and dashed lines represent fitted and 1:1 lines, respectively.

be dominated by WTD (figure S2, available at [stacks.iop.org/ERL/8/045003/mmedia](http://stacks.iop.org/ERL/8/045003/mmedia)), while the CH<sub>4</sub> sources seemed to be dominated by soil temperature (figure S3, available at [stacks.iop.org/ERL/8/045003/mmedia](http://stacks.iop.org/ERL/8/045003/mmedia)). For NEE, most of the study region had a negative NEE, or CO<sub>2</sub> sink, with a sink of atmospheric CO<sub>2</sub> up to  $-80 \text{ g C m}^{-2} \text{ yr}^{-1}$  during the 2000s. The West Siberia acted as a strong CO<sub>2</sub> sink, while other regions were weak sinks or small sources. The magnitude of NEE was comparable to other model simulations of northern terrestrial ecosystems (e.g., Wania *et al* 2009, Koven *et al* 2011). The spatial pattern of NEE was partly consistent with WTD (figure S2), since we only considered the heterotrophic respiration in unsaturated soils above WTD given that decomposition rates were very low under anaerobic conditions in saturated soils (Freeman *et al* 2001).

We evaluated our simulations with observations at field sites over the pan-Arctic (figure 3(a)). The comparison between the simulated and observed ALD at 155 circumpolar active layer monitoring (CALM) sites showed that our simulations underestimated ALD, especially for those soils with thick active layers (figure 3(b)). And the comparison between the simulated and observed mean daily CH<sub>4</sub> fluxes over the growing season (May–September) at 22 CH<sub>4</sub> flux sites (table S1, available at [stacks.iop.org/ERL/8/045003/mmedia](http://stacks.iop.org/ERL/8/045003/mmedia)) indicated that our simulations were able to well simulate the fluxes of CH<sub>4</sub> (figure 3(c)). However, our simulations overestimated the net fluxes of CO<sub>2</sub> (figure 3(d)), based on the comparison of the simulated and observed mean daily CO<sub>2</sub> fluxes (negative values indicate carbon sinks) over the growing season at 14 eddy covariance flux sites (table S2, available at [stacks.iop.org/ERL/8/045003/mmedia](http://stacks.iop.org/ERL/8/045003/mmedia)).

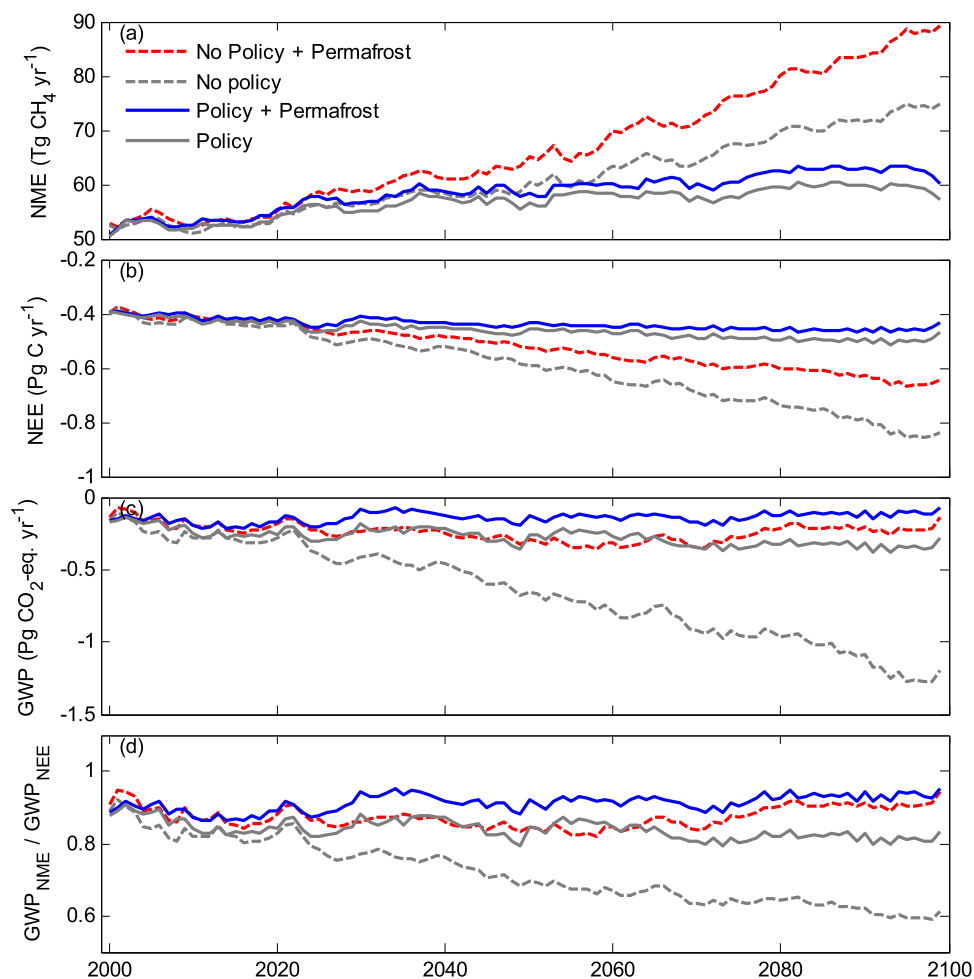


**Figure 4.** Annual net methane exchange (NME) (a), net ecosystem exchange (NEE) (b), global warming potential (GWP) (c), and the ratio of CH<sub>4</sub>- and CO<sub>2</sub>-induced GWP (d) over the pan-Arctic for the 21st century, under the no-policy (dashed lines) and policy (solid lines) scenarios. Gray lines indicate the simulations without considering the permafrost-thawing effect. Absolute values of GWP are used for the calculation of the ratios. A 5-year running mean is applied to all the curves.

For WTD, we compared our estimates (figure S2) with the simulations of global equilibrium WTD (Fan *et al* 2013) and found that the spatial pattern and magnitude of our estimates of WTD over the pan-Arctic was comparable with their results. The regions with shallow WTD well corresponded to major wetland regions over the pan-Arctic, including West Siberian Lowlands and Hudson Bay Lowlands.

### 3.2. Inter-annual variations of regional CH<sub>4</sub> and CO<sub>2</sub>

The annual regional total NME and NEE over the pan-Arctic exhibited a significant inter-annual variability over this century, and the difference in the estimates between no-policy and policy simulations increased over time, especially from the middle of this century (figures 4(a) and (b)). During the 2000s, the regional CH<sub>4</sub> source and CO<sub>2</sub> sink were estimated to be 53 Tg CH<sub>4</sub> yr<sup>-1</sup> and -0.4 Pg C yr<sup>-1</sup>, respectively. For the no-policy simulation, the magnitudes of CH<sub>4</sub> source and CO<sub>2</sub> sink were projected to be 85 Tg CH<sub>4</sub> yr<sup>-1</sup> and -0.7 Pg C yr<sup>-1</sup> during the 2090s, with annual changing rates of 0.38 Tg CH<sub>4</sub> yr<sup>-2</sup> and -2.8 Tg C yr<sup>-2</sup>, respectively (table 1). However, for the policy simulation, the annual

changing rates of regional CH<sub>4</sub> sources and CO<sub>2</sub> sinks were much smaller, about a quarter of the changing rates of the no-policy simulation (table 1). The big differences in the estimated NME and NEE resulted from the differential response of terrestrial ecosystems to various climate forcing and atmospheric CO<sub>2</sub> concentrations.

Our estimates of regional CO<sub>2</sub> sink under present climate conditions (-0.4 Pg C yr<sup>-1</sup>) was comparable to net carbon flux of this region based on previous model studies (-0.8–0 Pg C yr<sup>-1</sup>; McGuire *et al* 2009, Koven *et al* 2011, Schaphoff *et al* 2013), and contemporary regional CH<sub>4</sub> source (53 Tg CH<sub>4</sub> yr<sup>-1</sup>) was within the range of previous estimates (20–157 Tg CH<sub>4</sub> yr<sup>-1</sup>; Christensen *et al* 1996, Zhuang *et al* 2004, Petrescu *et al* 2010). For the no-policy simulation, the 60% increase in the projected CH<sub>4</sub> source by 2100 was comparable to the projected increase of future CH<sub>4</sub> emissions (51%) in northern Eurasia using similar climate change scenarios (Zhu *et al* 2011); and the projected regional CO<sub>2</sub> sink by the 2090s (-0.7 Pg C yr<sup>-1</sup>, a 75% increase over the 1990s level) was at the high end of the multi-model estimates of CO<sub>2</sub> sink (-0.3±0.3 Pg C yr<sup>-1</sup>; Qian *et al* 2010). Our simulations showed a consistent increase in regional

**Table 1.** Annual changing rate of key variables over the 21st century, under the no-policy and policy scenarios. The annual changing rates are determined as the slopes from a least square linear regression over the century, over the pan-Arctic. All estimates except those for GWP are statistically significant at  $P < 0.01$ .

	No-policy			Policy		
	Estimate	95% CI	$R^2$	Estimate	95% CI	$R^2$
Soil temperature <sup>a</sup> ( $^{\circ}\text{C yr}^{-1}$ )	0.042	(0.040, 0.043)	0.96	0.011	(0.010, 0.012)	0.91
Active layer depth ( $\text{cm yr}^{-1}$ )	0.538	(0.512, 0.564)	0.95	0.136	(0.118, 0.154)	0.70
Water table depth <sup>b</sup> ( $\text{cm yr}^{-1}$ )	-0.107	(-0.112, -0.101)	0.94	-0.036	(-0.041, -0.031)	0.69
NME ( $\text{Tg CH}_4 \text{ yr}^{-2}$ )	0.375	(0.361, 0.404)	0.91	0.113	(0.107, 0.119)	0.62
NPP ( $\text{Tg C yr}^{-2}$ )	-10.208	(-10.723, -9.754)	0.91	-2.542	(-2.654, -2.423)	0.70
$R_h$ ( $\text{Tg C yr}^{-2}$ )	8.154	(7.747, 8.558)	0.89	2.029	(1.928, 2.130)	0.76
NEE ( $\text{Tg C yr}^{-2}$ )	-2.771	(-2.911, -2.632)	0.90	-0.607	(-0.637, -0.576)	0.25
GWP ( $\text{Tg CO}_2\text{-eq. yr}^{-2}$ )	-0.779	(-0.827, -0.741)	0.05	0.543	(0.516, 0.571)	0.03

<sup>a</sup> Top-layer (0–5 cm) soil temperature.

<sup>b</sup> Mean water table depth during the growing season (May–Sep.).

net  $\text{CO}_2$  sink, suggesting that NPP will increase faster than soil decomposition in response to future climate warming over the century. This is not consistent with previous model studies (e.g., Koven *et al* 2011, Schaphoff *et al* 2013), which projected that, during the second half of this century, regional net  $\text{CO}_2$  sink will weaken and gradually turn into a source. The differential changing patterns of regional net  $\text{CO}_2$  sink in response to future climate change could be caused by different model assumptions and climate change scenarios. For example, the TEM used in our projections explicitly took into account the nitrogen limitation on plant. The inclusion of carbon–nitrogen interaction in the model projections might have greatly influenced how vegetation and soil carbon respond to future climate in the pan-Arctic.

### 3.3. Regional global warming potentials of $\text{CH}_4$ and $\text{CO}_2$

The spatial pattern of net GWP was a combination of the spatial variations of NME and NEE for both no-policy and policy simulations (figure 2 and figure S1 available at [stacks.iop.org/ERL/8/045003/mmedia](http://stacks.iop.org/ERL/8/045003/mmedia)). Those regions with high  $\text{CH}_4$  emissions tended to be a net GHG source (up to  $100 \text{ g CO}_2\text{-eq. m}^{-2} \text{ yr}^{-1}$ ), while other regions were generally a net GHG sink (up to  $-150 \text{ g CO}_2\text{-eq. m}^{-2} \text{ yr}^{-1}$ ) (figures 2(e) and (f)). The regional net GHG sink, the result of positive  $\text{CH}_4$ -GWP (GHG source) and negative  $\text{CO}_2$ -GWP (GHG sink), was estimated to be  $-0.2 \text{ Pg CO}_2\text{-eq. yr}^{-1}$  during the 2000s, and the annual GHG did not have a significant trend during the 21st century although the magnitude fluctuated over the century (figure 4(c)). Our estimate of the ratio of  $\text{CH}_4$  emissions to  $\text{CO}_2$  uptakes during the 2000s,  $\sim 10\%$  on a molar basis, was within the range of field observations (3–20% Whiting and Chanton 1993, 2001). Although  $\text{CH}_4$  source was relatively small in comparison with the  $\text{CO}_2$  sink, the  $\text{CH}_4$ -GWP offset  $\sim 90\%$  of  $\text{CO}_2$ -GWP (figure 4(d)), which highlighted the importance of  $\text{CH}_4$  in regional total radiative forcing. Over the 21st century, there was no significant trend for the ratio of  $\text{CH}_4$ -GWP to  $\text{CO}_2$ -GWP for both no-policy and policy simulations.

### 3.4. Effects of permafrost thawing on regional carbon budgets

Under future warming climate conditions, the thawing permafrost could lead to both enhanced decomposition and plant growth. The sign and magnitude of net carbon balance depends on the relative intensity of stimulation on soil decomposition and plant growth. In this study, two sets of model simulations, with the permafrost-switch on/off, were conducted, and the effect of permafrost thawing on regional carbon budgets was calculated as the difference between these two sets of simulations. Our results indicated that, by excluding the permafrost-thawing effect, our no-policy simulations showed a 8% decrease and a 14% increase in the absolute magnitude of regional  $\text{CH}_4$  source (figure 4(a)) and  $\text{CO}_2$  sink (figure 4(b)) over the 21st century, respectively, which implied that soil decomposition will be more intensified due to thawing permafrost, resulting in a net decrease in ecosystem carbon storage. The net losses of  $\text{CH}_4$  and  $\text{CO}_2$  associated with permafrost thawing were estimated to about  $0.6 \text{ Pg CH}_4$  and  $7.5 \text{ Pg C}$  over the century. Taken together, the net accumulated GHG sink were reduced by  $41.5 \text{ Pg CO}_2\text{-eq.}$  over the century, which was almost twice as the accumulated GHG sink ( $-24.1 \text{ Pg CO}_2\text{-eq.}$ ) simulated with a permafrost-thawing effect (figure 4(c)). Thus, the comparison between the no-policy simulations with and without the permafrost-thawing effect suggested that the thawing permafrost resulted in a 63% decrease in accumulated GHG sink over the 21st century. Compared with the no-policy simulation, there were small differences in the estimated carbon and GHG budgets between policy simulations with and without a permafrost-thawing effect.

Over the century, the simulated mean ALD, over the regions where permafrost still exists by 2100 (within the top 3 m), will change from  $\sim 1 \text{ m}$  during the 2000s to  $\sim 1.5 \text{ m}$  during the 2090s, and the annual changing rate of ALD ( $\sim 0.5 \text{ cm yr}^{-1}$ ) was comparable with the observed changes during recent two decades at CALM sites (Brown *et al* 2000). However, the underestimation of the simulated ALD (figure 3(b)) suggested that actual net carbon loss



due to permafrost thawing might be larger than what we have estimated (8.0 Pg C over the century). Our estimation of net carbon loss associated with permafrost thawing was lower than our previous estimates (Zhuang *et al* 2006), but our estimates did not consider other disturbances in this region (e.g., fires), which could also lead to higher carbon losses.

In addition, our calculations of net carbon loss due to permafrost thawing could be greatly influenced by the specification of the vertical distribution of SOC. To assess the influence of the choice of SOC profile data, we conducted one additional no-policy simulation using a biome-dependent SOC profile dataset (Jobbágy and Jackson 2000), which includes a global summary of vertical SOC distribution of each biome (SOC profiles for two major biomes in the pan-Arctic, boreal forest and tundra, were shown in figure S5, available at [stacks.iop.org/ERL/8/045003/mmedia](http://stacks.iop.org/ERL/8/045003/mmedia)). Compared to the previous no-policy simulations with SOC profile data derived from Harden *et al* (2012), this additional no-policy simulation, during the 2000s, showed a 12% decrease in CH<sub>4</sub> source (from 53 to 47 Tg CH<sub>4</sub> yr<sup>-1</sup>) and a 20% increase in CO<sub>2</sub> sink (from -0.4 to -0.5 Pg C yr<sup>-1</sup>), which together tripled the GHG sink (from -0.2 to -0.6 Pg CO<sub>2</sub>-eq. yr<sup>-1</sup>). However, in spite of the difference in the magnitude of carbon/GHG budgets, the changing patterns of NME, NEE and GWP from this additional no-policy simulation did not change in comparison with the previous simulations.

#### 4. Conclusions

Using a coupled hydrology–biogeochemistry model framework, the net carbon dynamics (CH<sub>4</sub> and CO<sub>2</sub>) and their combined GHG over the pan-Arctic were analyzed over the 21st century under two contrast climate change scenarios. Under present climate conditions, the region acted as a CH<sub>4</sub> source (53 Tg CH<sub>4</sub> yr<sup>-1</sup>) and a CO<sub>2</sub> sink (-0.4 Pg C yr<sup>-1</sup>), resulting in a net GHG sink of -0.2 Pg CO<sub>2</sub>-eq. yr<sup>-1</sup>. In response to future warming climate, both the CH<sub>4</sub> source and the CO<sub>2</sub> sink strengthened, but the net GHG sink did not show a significant trend. The increasing rates mainly depended on the climate change scenarios. Under the no-policy climate change scenario, the CH<sub>4</sub> source and the CO<sub>2</sub> sink were projected to increase 60% and 75% by 2100, respectively. The consistent increase in the CO<sub>2</sub> sink in our simulations suggested that NPP will increase faster than  $R_h$  in response to future climate warming over the 21st century. Although the amount of CH<sub>4</sub> emissions was small (~10% of the amount of carbon uptakes on a molar basis), they played an important role in affecting regional radiative forcing since CH<sub>4</sub>-GWP had offset almost all CO<sub>2</sub>-GWP over the century. Our simulations suggested that the thawing permafrost will enhance both CH<sub>4</sub> and CO<sub>2</sub> emissions, and the magnitude of future GHG sink will highly depend on whether a permafrost-thawing effect is included or not. The inclusion of a permafrost-thawing effect led to a 63% loss of GHG sink over the century.

The coupled hydrology–biogeochemistry model framework was operated at a fine spatial resolution, representing the critical effects of hydrological dynamics on GHG cycling of terrestrial ecosystems. The consideration of soil carbon distribution and thawing permafrost in quantification was another improvement to our previous quantification (e.g., Zhuang *et al* 2006). However uncertainties in the projection of GHG source/sink remained large due to two main sources. One the one hand, uncertainties came from the projection of future climate change, which itself was greatly affected by the climate policy implemented in the model and climate model parameterizations (e.g., climate sensitivity). In this study, we only considered the difference in climate policymaking (a reference case and a stabilization case), and a same climate model parameterization (median transient climate response) was applied in both cases (Webster *et al* 2012). One the other hand, large uncertainties could result from incomplete understanding of biogeochemical and physical processes in terrestrial ecosystems and the capacity of process-based models to represent underlying mechanisms at different temporal and spatial scales. Also, the choice of SOC profile data did influence our estimates especially for GWP, although it did not affect the changing patterns of carbon/GHG budgets over the century.

Although the CO<sub>2</sub>-fertilization, carbon–nitrogen interaction, and thawing permafrost were considered in the model to examine how CH<sub>4</sub> and CO<sub>2</sub> respond to climate change over the century, several other mechanisms, including fire disturbances (Carrasco *et al* 2006), changes in biome composition (Wilmking *et al* 2004), and cryoturbation in permafrost-affected soils (Bockheim 2007), can affect the quantification of pan-Arctic carbon balance and need to be included in future work. In particular, the CO<sub>2</sub> emissions from forest fires (~0.2 Pg C yr<sup>-1</sup>; Zhuang *et al* 2006) might have offset a half of net CO<sub>2</sub> sinks under present climate conditions. In addition, vegetation shifts (e.g., expansion of boreal forest Euskirchen *et al* 2009) and small-scale permafrost–hydrology interactions (e.g., thermokarst erosion van Huissteden *et al* 2011) are also needed to be considered in future assessment of carbon dynamics in the pan-Arctic.

#### Acknowledgments

We thank two anonymous reviewers for their thoughtful and constructive comments on the manuscript. The research is funded by a DOE SciDAC project and an Abrupt Climate Change project. This study is also supported through projects funded by the NASA Land Use and Land Cover Change program (NASA-NNX09AI26G), Department of Energy (DE-FG02-08ER64599), the NSF Division of Information and Intelligent Systems (NSF-1028291), and the NSF Carbon and Water in the Earth Program (NSF-0630319). This research is also in part supported by the Director, Office of Science, Office of Biological and Environmental Research of the US Department of Energy under Contract No. DE-AC02-05CH11231 as part of their Earth System Modeling Program.



## References

- ACIA 2004 *Impacts of a Warming Arctic: Arctic Climate Impact Assessment* (New York: Cambridge University Press) ([www.acia.uaf.edu](http://www.acia.uaf.edu))
- Bockheim J G 2007 Importance of cryoturbation in redistributing organic carbon in permafrost-affected soils *Soil Sci. Soc. Am. J.* **71** 1335–42
- Bohn T J and Lettenmaier D P 2010 Systematic biases in large-scale estimates of wetland methane emissions arising from water table formulations *Geophys. Res. Lett.* **37** L22401
- Bohn T J, Lettenmaier D P, Sathulur K, Bowling L C, Podest E, McDonald K C and Friborg T 2007 Methane emissions from western Siberian wetlands: heterogeneity and sensitivity to climate change *Environ. Res. Lett.* **2** 045015
- Brown J, Hinkel K M and Nelson F E 2000 The circumpolar active layer monitoring (CALM) program: research designs and initial results 1 *Polar Geogr.* **24** 166–258
- Carrasco J J, Neff J C and Harden J W 2006 Modeling physical and biogeochemical controls over carbon accumulation in a boreal forest soil *J. Geophys. Res.* **111** G02004
- Cherkauer K A, Bowling L C and Lettenmaier D P 2003 Variable infiltration capacity cold land process model updates *Glob. Planet. Change* **38** 151–9
- Christensen T R, Prentice I C, Kaplan J, Haxeltine A and Sitch S 1996 Methane flux from northern wetlands and tundra *Tellus B* **48** 652–61
- Clein J S, Kwiatkowski B L, McGuire A D, Hobbie J E, Rastetter E B, Melillo J M and Kicklighter D W 2002 Modelling carbon responses of tundra ecosystems to historical and projected climate: a comparison of a plot-and a global-scale ecosystem model to identify process-based uncertainties *Glob. Change Biol.* **6** 127–40
- Conrad R, Andreae M O and Schimel D S 1989 Control of methane production in terrestrial ecosystems *Exchange of Trace Gases Between Terrestrial Ecosystems and the Atmosphere* (Chichester: John Wiley & Sons) pp 39–58
- Davidson E A and Janssens I A 2006 Temperature sensitivity of soil carbon decomposition and feedbacks to climate change *Nature* **440** 165–73
- Euskirchen E S, McGuire A D, Chapin F S III, Yi S and Thompson C C 2009 Changes in vegetation in northern Alaska under scenarios of climate change, 2003–2100: implications for climate feedbacks *Ecol. Appl.* **19** 1022–43
- Euskirchen E S, McGuire A D, Kicklighter D W, Zhuang Q, Clein J S, Dargaville R J, Dye D G, Kimball J S, McDonald K C and Melillo J M 2006 Importance of recent shifts in soil thermal dynamics on growing season length, productivity, and carbon sequestration in terrestrial high-latitude ecosystems *Glob. Change Biol.* **12** 731–50
- Fan Y, Li H and Miguez-Macho G 2013 Global patterns of groundwater table depth *Science* **339** 940–3
- Freeman C, Ostle N and Kang H 2001 An enzymic ‘latch’ on a global carbon store *Nature* **409** 149
- Gorham E 1991 Northern peatlands: role in the carbon cycle and probable responses to climatic warming *Ecol. Appl.* **1** 182–95
- Harden J W et al 2012 Field information links permafrost carbon to physical vulnerabilities of thawing *Geophys. Res. Lett.* **39** L15704
- Hollesen J, Elberling B and Jansson P E 2011 Future active layer dynamics and carbon dioxide production from thawing permafrost layers in Northeast Greenland *Glob. Change Biol.* **17** 911–26
- Jobbágy E G and Jackson R B 2000 The vertical distribution of soil organic carbon and its relation to climate and vegetation *Ecol. Appl.* **10** 423–36
- Koven C D, Ringeval B, Friedlingstein P, Ciais P, Cadule P, Khvorostyanov D, Krinner G and Tarnocai C 2011 Permafrost carbon-climate feedbacks accelerate global warming *Proc. Natl Acad. Sci.* **108** 14769–74
- Lammers R B, Shiklomanov A I, Vörösmarty C J, Fekete B M and Peterson B J 2001 Assessment of contemporary Arctic river runoff based on observational discharge records *J. Geophys. Res.* **106** 3321–34
- Liang X, Lettenmaier D P, Wood E F and Burges S J 1994 A simple hydrologically based model of land surface water and energy fluxes for general circulation models *J. Geophys. Res.* **99** 14415–28
- Lu X and Zhuang Q 2012 Modeling methane emissions from the Alaskan Yukon River basin, 1986–2005, by coupling a large-scale hydrological model and a process-based methane model *J. Geophys. Res.* **117** G02010
- Mack M C, Schuur E A G, Bret-Harte M S, Shaver G R and Chapin F S 2004 Ecosystem carbon storage in Arctic tundra reduced by long-term nutrient fertilization *Nature* **431** 440–3
- McGuire A D, Anderson L G, Christensen T R, Dallimore S, Guo L, Hayes D J, Heimann M, Lorenson T D, Macdonald R W and Roulet N 2009 Sensitivity of the carbon cycle in the Arctic to climate change *Ecol. Monogr.* **79** 523–55
- McGuire A D et al 2010 An analysis of the carbon balance of the Arctic basin from 1997 to 2006 *Tellus B* **62** 455–74
- Melton J R et al 2013 Present state of global wetland extent and wetland methane modelling: conclusions from a model inter-comparison project (WETCHIMP) *Biogeosciences* **10** 753–88
- Osterkamp T E, Jorgenson M T, Schuur E A G, Shur Y L, Kanevskiy M Z, Vogel J G and Tumskey V E 2009 Physical and ecological changes associated with warming permafrost and thermokarst in interior Alaska *Permafrost Periglac. Process.* **20** 235–56
- Petrescu A M R, van Beek L P H, van Huissteden J, Prigent C, Sachs T, Corradi C A R, Parmentier F J W and Dolman A J 2010 Modeling regional to global CH<sub>4</sub> emissions of boreal and Arctic wetlands *Glob. Biogeochem. Cycles* **24** GB4009
- Prinn R, Jacoby H, Sokolov A, Wang C, Xiao X, Yang Z, Eckhaus R, Stone P, Ellerman D and Melillo J 1999 Integrated global system model for climate policy assessment: feedbacks and sensitivity studies *Clim. Change* **41** 469–546
- Qian H, Joseph R and Zeng N 2010 Enhanced terrestrial carbon uptake in the northern high latitudes in the 21st century from the coupled carbon cycle climate model intercomparison project model projections *Glob. Change Biol.* **16** 641–56
- Raich J W, Rastetter E B, Melillo J M, Kicklighter D W, Steudler P A, Peterson B J, Grace A L, Moore B III and Vörösmarty C J 1991 Potential net primary productivity in South America: application of a global model *Ecol. Appl.* **1** 399–429
- Reilly J M, Prinn R G, Harnisch J, Fitzmaurice J, Jacoby H D, Kicklighter D W, Stone P H, Sokolov A P and Wang C 1999 Multi-gas assessment of the Kyoto Protocol *Nature* **401** 549–55
- Romanovsky V E, Sazonova T S, Balobaev V T, Shender N I and Sergueev D O 2007 Past and recent changes in air and permafrost temperatures in eastern Siberia *Glob. Planet. Change* **56** 399–413
- Schaphoff S, Heyder U, Ostberg S, Gerten D, Heinke J and Lucht W 2013 Contribution of permafrost soils to the global carbon budget *Environ. Res. Lett.* **8** 014026
- Schulze E D, Lloyd J, Kelliher F M, Wirth C, Rebmann C, Lühker B, Mund M, Knohl A, Milyukova I M and Schulze W 2001 Productivity of forests in the Eurosiberian boreal region and their potential to act as a carbon sink—a synthesis *Glob. Change Biol.* **5** 703–22

- Schuur E A G *et al* 2008 Vulnerability of permafrost carbon to climate change: implications for the global carbon cycle *Bioscience* **58** 701–14
- Segers R 1998 Methane production and methane consumption: a review of processes underlying wetland methane fluxes *Biogeochemistry* **41** 23–51
- Sokolov A P, Stone P H, Forest C E, Prinn R, Sarofim M C, Webster M, Paltsev S, Schlosser C A, Kicklighter D and Dutkiewicz S 2009 Probabilistic forecast for twenty-first-century climate based on uncertainties in emissions (without policy) and climate parameters *J. Clim.* **22** 5175–204
- Solomon S, Qin D, Manning M, Chen Z, Marquis M, Averyt K B, Tignor M and Miller H L 2007 *Climate Change 2007: The Physical Science Basis: Working Group I Contribution to the Fourth Assessment Report of the Intergovernmental Panel on Climate Change* (Cambridge: Cambridge University Press)
- Su F, Adam J C, Bowling L C and Lettenmaier D P 2005 Streamflow simulations of the terrestrial Arctic domain *J. Geophys. Res.* **110** D08112
- Su F, Adam J C, Trenberth K E and Lettenmaier D P 2006 Evaluation of surface water fluxes of the pan-Arctic land region with a land surface model and ERA-40 reanalysis *J. Geophys. Res.* **111** D05110
- Tang J, Zhuang Q, Shannon R D and White J R 2010 Quantifying wetland methane emissions with process-based models of different complexities *Biogeosciences* **7** 3817–37
- Tarnocai C, Canadell J G, Schuur E A G, Kuhry P, Mazhitova G and Zimov S 2009 Soil organic carbon pools in the northern circumpolar permafrost region *Glob. Biogeochem. Cycles* **23** GB2023
- van Huissteden J, Berrittella C, Parmentier F J W, Mi Y, Maximov T C and Dolman A J 2011 Methane emissions from permafrost thaw lakes limited by lake drainage *Nature Clim. Change* **1** 119–23
- Walter B P, Heimann M and Matthews E 2001 Modeling modern methane emissions from natural wetlands 1. Model description and results *J. Geophys. Res.* **106** 34189–206
- Walter K M, Zimov S A, Chanton J P, Verbyla D and Chapin F S 2006 Methane bubbling from Siberian thaw lakes as a positive feedback to climate warming *Nature* **443** 71–5
- Wania R, Ross I and Prentice I C 2009 Integrating peatlands and permafrost into a dynamic global vegetation model: 2. Evaluation and sensitivity of vegetation and carbon cycle processes *Glob. Biogeochem. Cycles* **23** GB3015
- Webster M, Forest C, Reilly J, Babiker M, Kicklighter D, Mayer M, Prinn R, Sarofim M, Sokolov A and Stone P 2003 Uncertainty analysis of climate change and policy response *Clim. Change* **61** 295–320
- Webster M, Sokolov A P, Reilly J M, Forest C E, Paltsev S, Schlosser A, Wang C, Kicklighter D, Sarofim M and Melillo J 2012 Analysis of climate policy targets under uncertainty *Clim. Change* **112** 569–83
- Whiting G J and Chanton J P 1993 Primary production control of methane emission from wetlands *Nature* **364** 794–5
- Whiting G J and Chanton J P 2001 Greenhouse carbon balance of wetlands: methane emission versus carbon sequestration *Tellus B* **53** 521–8
- Wilmking M, Juday G P, Barber V A and Zald H S J 2004 Recent climate warming forces contrasting growth responses of white spruce at treeline in Alaska through temperature thresholds *Glob. Change Biol.* **10** 1724–36
- Zhu X, Zhuang Q, Chen M, Sirin A, Melillo J, Kicklighter D, Sokolov A and Song L 2011 Rising methane emissions in response to climate change in Northern Eurasia during the 21st century *Environ. Res. Lett.* **6** 045211
- Zhuang Q, McGuire A D, O'Neill K P, Harden J W, Romanovsky V E and Yarie J 2002 Modeling soil thermal and carbon dynamics of a fire chronosequence in interior Alaska *J. Geophys. Res.* **107** 8147
- Zhuang Q, Melillo J M, Kicklighter D W, Prinn R G, McGuire A D, Steudler P A, Felzer B S and Hu S 2004 Methane fluxes between terrestrial ecosystems and the atmosphere at northern high latitudes during the past century: a retrospective analysis with a process-based biogeochemistry model *Glob. Biogeochem. Cycles* **18** GB3010
- Zhuang Q, Melillo J M, Sarofim M C, Kicklighter D W, McGuire A D, Felzer B S, Sokolov A P, Prinn R G, Steudler P A and Hu S 2006 CO<sub>2</sub> and CH<sub>4</sub> exchanges between land ecosystems and the atmosphere in northern high latitudes over the 21st century *Geophys. Res. Lett.* **33** L17403